arXiv:0708.3167v1 [cond-mat.supr-con] 23 Aug 2007

Asymmetric Fermi superfluid with different atomic species in a harmonic trap

C.-H. Pao and Shin-Tza Wu
Department of Physics, National Chung Cheng University, Chiayi 621, Taiwan

S.-K. Yip
Institute of Physics, Academia Sinica, Nankang, Taipei 115, Taiwan

(Dated: August 20, 2007)

We study the dilute fermion gas with pairing between two species and unequal concentrations in a harmonic trap using the mean field theory and the local density approximation. We found that the system can exhibit a superfluid shell structure sandwiched by the normal fermions. This superfluid shell structure occurs if the mass ratio is larger then certain critical value which increases from the weak-coupling BCS region to the strong-coupling BEC side. In the strong coupling BEC regime, the radii of superfluid phase are less sensitive to the mass ratios and are similar to the case of pairing with equal masses. However, the lighter leftover fermions are easier to mix with the superfluid core than the heavier ones. A partially polarized superfluid can be found if the majority fermions are lighter, whereas phase separation is still found if they are heavier.

PACS numbers: 03.75.Ss, 05.30.Fk, 34.90.+q

I. INTRODUCTION

Recently experimental progress has raised strong interest in studying the superfluid pairing in the ultracold Fermi gases [1]. Through the Feshbach resonance [2], the effective interaction between atoms can be tuned over a wide range. This technique led us to investigate the crossover between the condensation of weak-coupling Cooper pairs and the Bose-Einstein condensation (BEC) of strong-coupling tightly bound pairs[3]. More recently, two experimental groups extend a step further by controlling the polarization of the two states Fermi gases [4] and open a new era for studying the imbalanced Fermi gases, which is a topic related to many interesting areas from condensed-matter physics, nuclear physics, to quark matter [5].

Stimulated by these excellent experiments of the imbalanced Fermi gases, there are intense theoretical works in the past two years. For a homogeneous system, the smooth crossover is known to be destroyed when the populations of the fermions are unequal [6, 7, 8, 9]. In an inhomogeneous case, *e.g.* in a harmonic trap potential, phase separation occurs near resonance with the superfluid is at the trap center surrounding by the normal phase [10, 11, 12, 13, 14, 15]. Finite temperature phase diagrams and density profiles are also studied in this imbalanced system recently [16, 17, 18, 19, 20].

Feshbach resonances between different atomic species have also been reported [21] and the pairing of unequal masses fermions has received theoretical interest. Focusing on the pairing of ^{6}Li-^{40}K mixtures, the phase diagram was studied both in a homogeneous system [22] and in a trap potential [23]. Other works on a general unequal mass ratios, including the analytic results at unitary limit [24] and the evolution of the tricritical point [25] have also been studied recently.

In this paper, we study the density profiles for unequal mass fermions in harmonic traps at zero temperature. Within the local density approximation, or Thomas-Fermi approximation, we solve the BCS gap equation self-consistently at fixed total number of particles and polarization. We analyze the density profiles from unpolarized to highly imbalanced phases. Due to the large number of possible atoms (e.g. ^{2}H, ^{3}He* [26], ^{6}Li, ^{40}K, ^{87}Sr [27], and ^{173}Yb [28]), we study general mass ratios from 0.1 to 10 and particular $(k_Fa)^{-1} = -0.5$, 0, and 1.0 as the representative scenarios for weak-couping BCS, on resonance, and strongly paired BEC regimes. We found, on the weak coupling BCS side, the superfluid can form a shell structure sandwiched between normal fermions for large mass ratios. At resonance, the normal fluids can be either partially or completely polarized, depending on the mass ratios. On the BEC side, the radii of superfluid core are insensitive to the mass ratios. A partially polarized superfluid can be found if the majority fermions are lighter, whereas phase separation is still found if they are heavier. We also report the axial density profiles of the population difference and discuss the significant differences compared to the pairing with equal masses.

Mismatch Fermi surfaces may result a different ground state than phase separations, in particular the so-called Fulde-Ferrel-Larkin-Ovchinnikov (FFLO) phase [29]. In this paper, we leave out this possible FFLO phase for future investigation [30].

The remainder of this paper is organized as follows: In Sec. II we briefly review the mean-field approximation for the dilute two states of fermion atoms with unequal masses. We present our numerical results along with discussion, in Sec. III. Finally, in Sec. IV, we conclude with a briefly summary.

II. FORMALISM:

We start from the two-component fermion system across a wide Feshbach resonance which may be described

by an effective one-channel Hamiltonian:

$$H = \sum_{\mathbf{k},\sigma} \xi_\sigma(\mathbf{k}) c^\dagger_{\mathbf{k},\sigma} c_{\mathbf{k},\sigma} + g \sum_{\mathbf{k},\mathbf{k}',\mathbf{q}} c^\dagger_{\mathbf{k}+\mathbf{q},h} c^\dagger_{\mathbf{k}'-\mathbf{q},l} c_{\mathbf{k}',l} c_{\mathbf{k},h} \ , \quad (1)$$

where $\xi_\sigma(\mathbf{k}) = \hbar^2 k^2/2m_\sigma - \mu_\sigma$, g the bare coupling strength, and the index σ runs over the two species (h and l). Within the BCS mean field approximation, the excitation spectrum in a homogeneous system for each species is (see e.g. [31] for details)

$$E_\sigma(\mathbf{k}) = \frac{\xi_\sigma(\mathbf{k}) - \xi_{-\sigma}(\mathbf{k})}{2} + \sqrt{\left(\frac{\xi_\sigma(\mathbf{k}) + \xi_{-\sigma}(\mathbf{k})}{2}\right)^2 + \Delta^2} \ . \quad (2)$$

where $-h \equiv l$. In order to include the pairing between unequal masses, we use m_h (m_l) to represent the mass of each component with heavier (lighter) mass and rewrite the dispersion relation of Eq. (2) as

$$E_{h,l}(\mathbf{k}) = \mp \left[\frac{\hbar^2 k^2}{4m_r}\frac{\gamma-1}{\gamma+1} + h\right] + \sqrt{\left(\frac{\hbar^2 k^2}{4m_r} - \mu\right)^2 + \Delta^2} \ , \quad (3)$$

with the reduced mass m_r, the mass ratio $\gamma = m_h/m_l$, the chemical potential difference $h \equiv (\mu_h - \mu_l)/2$ and the average chemical potential $\mu \equiv (\mu_h + \mu_l)/2$.

For the fermion gases in a harmonic trap, the system can be treated as homogeneous locally if the number of particles are sufficiently large. Within this local density approximation, the densities at position $\vec{r}$ depends only on the local effective chemical potentials

$$\mu_{h,l}(\vec{r}) = \mu^0_{h,l} - V_{h,l}(\vec{r}) \quad (4)$$

where $V_{h,l}(\vec{r})$ is the trap potential for the species h or l. To simplify our presentation we shall consider an isotropic trap where the potential depends only on the radius r.

The density profiles can be found via

$$N_s(r) = N_h(r) + N_l(r) = \int \frac{d^3k}{(2\pi)^3} \left[1 + 2\left(\frac{\hbar^2 k^2}{4m_r} - \mu(r)\right)\frac{f(E_h) - f(-E_l)}{E_h + E_l}\right] \quad (5)$$

$$N_d(r) = N_h(r) - N_l(r) = \int \frac{d^3k}{(2\pi)^3}\Big[f(E_h) - f(E_l)\Big] \ , \quad (6)$$

with f is the Fermi function. The total number of particles $N = \int d^3r N_s(r)$ and the polarization of the system is defined as

$$P \equiv \frac{1}{N}\int d^3r N_d(r) \ . \quad (7)$$

Note that the polarization is positive (negative) for a system with the majority are heavier (lighter).

Now the pairing field Δ depends on position also. In the local density approximation, it obeys an equation similar to the homogeneous case [6, 31]:

$$-\frac{m_r}{2\pi a}\Delta(r) = \Delta(r)\int \frac{d^3k}{(2\pi)^3}\left[\frac{1 - f(E_h) - f(E_l)}{E_h + E_l} - \frac{2m_r}{\hbar^2 k^2}\right] \ . \quad (8)$$

For a given s-wave scattering length a, we solve equations (5), (6) and (8) self-consistently for fixed total number of particles N and polarization P. The solutions of the "gap equation" (8) may not be unique and the physical solution is determined by the condition of minimum free energy among the multiple solutions. The detailed procedure can be found in reference [10].

To avoid extra complications, we confine ourselves to the case where the trapping potential is harmonic. We further assume that it is identical for the two species. Thus $V(r) = \frac{1}{2}\alpha_{h,l} r^2$ with $\alpha_h = \alpha_l = \alpha$. This would occur, for example, if both species are trapped magnetically and if the fermions have identical magnetic moments, or when the fermions are trapped optically with different lasers of appropriate intensities and detunings. In this case, within the local density approximation, the density profiles for the same polarization P but different total particle numbers are related to each other via simple scaling. This allow us to present our results in a manner which is independent of the total particle numbers (see below). When the trap potentials are unequal, many other scenarios can occur. We shall leave the investigation of this more complicated case to the future.

III. RESULTS

In this section, we investigate the density profiles for various polarizations, mass ratios and coupling strengths from positive detuning BCS superfluid to negative detuning BEC side. With the aid of density profiles, we plot the superfluid phase diagram in a harmonic trap for different mass ratios. Finally, we also evaluate the axial density profiles of the population difference and discuss the effect due to the mass ratios at different coupling strengths.

We begin by examining the radial density profiles for the mass ratios $\gamma = 2.0$, and 5.0 with various polarizations from 0.8 (majority are heavier) to -0.8 (majority are lighter). The densities $N(r)$ are normalized to the total density at the trap center and distances are normalized to the Thomas-Fermi radius of the non-interacting majority gas of the same atom number. In Figs. 1–3, we plot the radial density profiles at three different coupling strengths with $(k_F a)^{-1} = 0$ (the unitary limit), 1.0 (strong coupling BEC), and -0.5 (weak-coupling BCS).

In the unitary limit, the system exhibits a superfluid core surrounded by normal fermions for $\gamma = 2.0$ [Fig.

1(a)–(e)]. The density profiles are qualitatively the same between positive and negative polarizations. For example, for the large polarizations $P = \pm 0.8$ [Fig. 1(a) and (e)], we found that the superfluid core of the majority are lighter is only slightly larger than that of the majority are heavier. However, for $P > 0$ there are small amounts of minority in the normal region but it is completely polarized for the case of $P < 0$. The above results are in accordance with Fig. 2 of reference [24]. At the interface between the superfluid and the normal fluid, the two phases are in equilibrium and the local polarization of the latter phase should be given by the same value obtained from our earlier bulk calculations there. The asymmetry between the positive and negative polarizations becomes more obvious for larger mass ratio, *e.g.*, $\gamma = 5$ in Fig. 1(f)–(j). In Fig. 1(g) and (h), the superfluid is sandwiched between two regions with normal fermions. The inner core is a normal state with heavy particles being the majority, whereas the outer normal shell consists purely the lighter species [32]. The superfluid shell extends toward the trap center as the polarization decreases from large positive value. At equal populations [Fig. 1(h)], we found the system is still phase separated into normal polarized fermions and unpolarized superfluid regions. This is quite different compare to the equal or small mass ratio (*e.g.*, $\gamma = 2.0$ here) cases which the system is superfluid for the entire trap [33].

The existence of this normal fluid core can be understood as due to the fact that this normal fluid has a *higher* number density than the paired superfluid at this mass ratio [24], and hence it "sinks" towards the center of the trap where the trap potential is the minimum (recall that we have assumed $\alpha_h = \alpha_l$). We note also here that, as shown in Fig 1, the total number density is a decreasing function of r. In fact, the results of [24] then indicate that the critical mass ratio above which for the occurrence of a normal state core with a superfluid shell is $\gamma^* = 3.9$ at resonance (see Fig. 3 of reference [24]).

In Fig. 2, we plot the radial density profiles for $\gamma = 2.0$ and 5.0 with $(k_F a)^{-1} = 1.0$. At this coupling strength, the radii of the superfluid core are found to be only very weakly dependent on the mass ratio or the sign of polarization. However, the phases are very different depending on whether the majority particles are the heavier or lighter ones. We found that all particles are paired for a unpolarized case ($P = 0$). When the majority fermions are heavier ($P > 0$), the system contains an unpolarized superfluid core with a surrounding outside shell of normal fluid consisting of the majority particles alone. Thus phase separation occurs in this case between the completely paired superfluid and the completely polarized normal phase. On the other hand, when the majority is light ($P < 0$), the equally paired superfluid core at the trap center is surrounded by a partially polarized superfluid mixture phase, with a normal shell occupying the outermost region of the trap. This normal shell is again found to be completely polarized. In this strongly paired BEC regime, all minority particles exist only within the bound pairs and thus within the superfluid phase(s) only. Note also that the coupling strength is now strong enough so that the superfluid always has a higher density than the normal phase, and the superfluid shell structure found at resonance no longer appears here.

In the BCS regime, since the pairing interaction is weak, the density profiles are most easily understood by first considering the normal state density profiles. We note here that due to the different mass ratios and unequal populations, these two profiles have very different dependence on the position r. In the presence of the weak interaction, pairing would occur only at locations where the local populations are almost equal, or when the density is sufficiently large so that the effective interaction is sufficiently strong. This results in a rich structures in the density profiles as we shall show. In Fig. 3, we plot the radial density profiles for the coupling strength $(k_F a)^{-1} = -0.5$ and mass ratios $\gamma = 2.0$ and 5.0. The symmetry between the positive and negative polarization is lost even for $\gamma = 2.0$ [Fig. 3(a)–(e)]. At large populations imbalances (*e.g.*, $P = \pm 0.8$ in Fig. 3), a superfluid core still forms for majority are lighter but only normal fermions exist in the trap for majority are heavier. Similar to the unitary limit, the system exhibits a superfluid core surrounded by normal fermions for a wide range of polarization at $\gamma = 2.0$. But at larger γ [Fig. 3(f)–(j)], the heavier normal fermions prefer to stay in the trap center and the superfluid phase is outside this normal phase. We also found that the superfluid shell grows as the population of lighter fermions increase [Fig. 3(g)–(i)]. This superfluid shell structure finally reaches the trap center and all normal fermions are forced into the outside shell. We would like to emphasize that the shell structure of the normal fermions are not the same as the cases in the unitary limit. In Fig. 1(g) and (i), the outside shell of the normal fermions are fully polarized but both components of fermions exist here for this weak-coupling side.

In Fig. 3(b), we found that the density profile contains two regions of superfluid and polarized fermions. As mentioned, a stable superfluid occurs when either the density of each component of fermion is large or the size of Fermi surfaces of these two fermion states are approximately equal. In Fig. 4, we enlarge the Fig. 3(b) and plot the density profiles of both components of the non-interacting fermions also. It shows that the superfluid shell just occurs near the crossing of these two non-interacting density profiles since the superfluid gap is easier to open near this point [23]. On the other hand, the density is large enough such that the superfluid phase is again stable at the trap center.

In view of the rich structure on the BCS side, we turn next to the phase diagram of the superfluid in a trap potential in this regime. We plot the phase diagrams in Fig. 5 for several different mass ratios with the same coupling strength $(k_F a)^{-1} = -0.5$. In Fig. 5(a) ($\gamma = 1$), the superfluid phase extends to the entire trap at the un-

polarized system ($P = 0$) and is symmetric about this point. For $\gamma > 1$, the fermion paired between different masses, the maximum radius of the superfluid phase moves toward negative polarization where the majority of the system are lighter. The symmetric phase diagram does not hold anymore. At increasing mass ratio ($\gamma \gtrsim 3$), we found that the superfluid at the trap center is not stable for the positive polarization. Instead, the superfluid phase occurs at some finite radius for the parameters we studied in Fig. 5(b)–(e). The shell structure of the superfluid is present for a wide range of polarizations as the mass ratio γ increases. In Fig. 5(b), $\gamma = 2.0$, the superfluid phase is split into two regions by the normal fermions and vice versa for $0 \lesssim P \lesssim 0.4$, corresponding to the concentric structure we discuss in Fig. 3(b) above. Note that, the mass ratios in Fig. 5(b), (c), and (d) correspond to the mixtures of ^{3}He*–^{6}Li, ^{2}H–^{6}Li and ^{6}Li–^{40}K.

In Fig. 6, we also plot the superfluid phase for three different coupling strengths with $\gamma = 5.0$. The superfluid shell structure still exists at the unitary limit [Fig. 6(b)] but only for positive polarizations. On the BEC side [Fig. 6(c)], the symmetry of the superfluid phase about the equal population almost regains. However, there is a region where the superfluid and leftover fermions are mixed with each other for $P < 0$. For $P > 0$, there is only unpolarized superfluid phase and the system is phase separated.

Lastly we would like to examine the axial density profiles of the population difference defined as [10]:

$$N_d(z) \;=\; \int dxdy\big[N_h(\vec{r}) - N_l(\vec{r})\big] \;. \qquad (9)$$

In Fig. 7, we plot these results for $(k_F a)^{-1} = -0.5$, 0.0 and 1.0 and the mass ratios ($\gamma' \equiv m_{majoity}/m_{minority}$) between majority and minority species from 0.1 to 10.0 at polarization $|P| = 0.2$.

On the BCS side [Fig. 7(a)] and the unitary limit [Fig. 7(b)], the horizontal segments of each curve $N_d(z)$ correspond to the unpolarized superfluid. For the cases of majority lighter ($\gamma' \lesssim 0.2$), we found that the minority (with heavier mass) crowd into the trap center and have higher population than the majority locally. Thus, the axial density profiles show the dip structure in the trap center. In the other limit, $\gamma' \gtrsim 5.0$ (the majority are heavier), the peak of the axial density profile appears right at the trap center.

At the unitary limit [Fig. 7(b)], the axial density profiles are similar except for $\gamma' = 5.0$ and 10.0. This is the results where the heavier fermions have larger populations near the trap center and the superfluid shows a shell structure as we discuss in Fig. 1.

On the strong coupling BEC side [Fig. 7(c)], the structures of all of the curves are similar for different mass ratios. The radii of the superfluid core in this coupling strength are not sensitive to γ' either. The only difference is that $N_d(z)$ are smooth at the phase boundary for the cases of the majority are lighter but there exist kinks for the cases of the majority are heavier . It is consistent with the results in Fig. 2 that the lighter fermions are easier to mix with superfluid than the heavier ones.

IV. CONCLUSION

We have studied the two-component fermion system with unequal masses and populations across Feshbach resonance. For the pairing with unequal species, the superfluid can be sandwiched by the normal fermions and form a superfluid shell structure. This superfluid shell structure is easier to observe on the weak-coupling BCS side or at the unitary limit with large mass ratios (*i.e.*, in the systems of ^{40}K–^{173}Yb, ^{6}Li–^{40}K, or ^{6}Li–^{87}Sr[27]). For a given mass ratios, this superfluid shell extends toward the trap center as the population of lighter fermions increase.

In the strong coupling BEC regime, the superfluid phase is less sensitive to the mass ratios and is similar to the case of pairing with equal masses. However, lighter leftover fermions are easier to penetrate into the superfluid core than the heavier ones. At coupling strength $(k_F a)^{-1} = 1.0$, phase separation between the completely polarized superfluid and the completely polarized normal phase occurs for the majority are heavier. On the other hand, the equal paired superfluid core at the trap center is surrounded by a partially polarized superfluid mixture phase and a normal shell occupying the outmost region of the trap.

Acknowledgments

This research was supported by the National Science Council of Taiwan under grant numbers NSC95-2112-M-194-011 (CHP), NSC95-2112-M-194-003 (STW) and NSC95-2112-M-001-054 (SKY).

[1] C. A. Regal, M. Greiner, and D.S. Jin, Phys. Rev. Lett. **92**, 040403 (2004); M. W. Zwierlein *et al.*, *ibid.* **92**, 120403 (2004); J. Kinast, S.L. Hemmer, M.E.Gehm, A. Turlapov, and J.E. Thomas, *ibid.* **92**, 150402 (2004); T. Bourdel *et al*, *ibid.* **93**, 050401 (2004); C. Chin *et al.*, Science **305**, 1128 (2004); and references therein.

[2] E. Tiesinga, B. J. Verhaar, H. T. C. Stoof, Phys. Rev. A **47**, 4114 (1993); S. Inouye *et al.*, Nature **392**, 151 (1998); P. Courteille, R.S. Freeland, D.J. Heinzen, F.A. van Abeelen, and B.J. Verhaar, Phys. Rev. Lett. **81**, 69 (1998); J. L. Roberts *et al.*, *ibid.* **81**, 5109 (1998).

[3] D. M. Eagles, Phys. Rev. **186**, 456 (1969); A. J. Leggett

in *Modern Trends in the theory of condensed matter*, edited by A. Pekalski and J. Przystawa (Springer-Verlag, Berlin, 1980).

[4] M.W. Zwierlein, A. Schirotzek, C.H. Schunck, and W. Ketterle, Science **311**, 492 (2006); G. B. Partridge, W. Li, R.I. Kamar, Y. Liao and R.G. Hulet *ibid.* **311**, 503 (2006); Y. Shin, M.W. Zwierlein, C.H. Schunck, A. Schirotzek, and W. Ketterle, Phys, Rev. Lett. **97**, 030401 (2006); C.H. Schunck, Y.Shin, A. Schirotzek, M.W. Zwierlein, and and W. Ketterle, Science **316**, 867 (2007); G.B. Partridge, Wenhui Li, Tean-an Liao, R.G. Hulet, M. Haque, and H. T. C. Stoof, *ibid.* **97** 190407 (2006).

[5] MMichael McNeil Forbes, E. Gubankova, W. V. Liu, and Frank Wilczek, Phys. Rev. Lett. **94**, 017001 (2005); R. Casalbuoni and G. Nardulli, Rev. Mod. Phys. **76**, 263 (2004) and references therein.

[6] C.-H. Pao, Shin-Tza Wu, and S.-K. Yip, Phys. Rev. B**73**, 132506 (2006); **74**, 189901(E) (2006).

[7] D.E. Sheehy and L. Radzihovsky, Phys. Rev. Lett. **96**, 060401 (2006).

[8] D.E. Sheehy and L. Radzihovsky, Ann. Phys. in press (cond-mat/0607803).

[9] D. T. Son and M. A. Stephanov, Phys. Rev. A**74**, 013614 (2006).

[10] C.-H. Pao and S.-K. Yip, J. Phys. : Condens. Matter **18**, 5567 (2006).

[11] W. Yi and L.M. Duan Phys. Rev. A **73**, 031604(R) (2006).

[12] T.N. De Silva and E.J. Mueller, Phys. Rev. A**73**, 051602(R) (2006); Phys. Rev. Lett. **97**, 070402 (2006).

[13] M. Haque and H.T.C. Stoof, Phys. Rev. A**74**, 011602(R) (2006); Phys. Rev. Lett. **98**, 260406 (2007).

[14] F. Chevy, Phys. Rev. Lett. **96**, 130401 (2006).

[15] C. Lobo, A. Recati, S. Giorgini and S. Stringari, Phys. Rev. Lett. **97**, 200403 (2006).

[16] K.B. Gubbels, M.W.J. Romans, and H.T.C. Stoof, Phys. Rev. Lett. **97**, 210402 (2006).

[17] R. Sensarma, W. Schnedier, R. B. Diener and M. Randeria, e-print arXiv:cond-mat/0706.1741.

[18] Chih-Chun Chien, Qijin Chen, Yan He, and K. Levin, Phys. Rev. Lett. **97**, 090402 (2006); *ibid.* **98**, 110404 (2007); Qijin Chen, C.A. Regal, D.S. Jin, and K. Levin, Phys. Rev. A **74**, 011601(R) (2006).

[19] M.M. Parish, F.M. Marchetti, A. Lamacraft, and B.D. Simons, Nature Physics 3, 124 (2007).

[20] Chi-Ho Cheng and S. K. Yip, Phys. Rev. B **75**, 014526 (2007).

[21] C. A. Stan, M. W. Zwierlein, C. H. Schunck, S. M. F. Raupach, and W. Ketterle, Phys. Rev. Lett. **93**, 143001 (2004); S. Inouye, J. Goldwin, M. L. Olsen, C. Ticknor, J. L. Bohn, and D. S. Jin, *ibid.* **93**, 183201 (2004).

[22] M. Iskin and C. A. R. Sa de Melo, Phys. Rev. lett. **97**, 100404 (2006).

[23] G.-D. Lin, W. Yi, and L.-M. Duan, Phys. Rev. A**74**, 031604(R) (2006).

[24] Shin-Tza Wu, C.-H. Pao, and S.-K. Yip, Phys. Rev. B**74** 224504 (2006).

[25] M.M. Parish, F.M. Marchetti, A. Lamacraft, and B.D. Simons, Phys. Rev. Lett. **98**. 160402 (2007).

[26] J. M. McNamara, T. Jeltes, A. S. Tychkov, W. Hogervorst and W. Vassen, Phys. Rev. Lett. **97**, 080404 (2006).

[27] Current project at University of Innsbruck: Heteronuclear molecules of fermionic lithium, potassium and strontium (FeLiKx). Please see website at <http://www.uibk.ac.at/exphys/ultracold/>

[28] T. Fukuhara, Y. Takasu, M. Kumakura and Y. Takahashi, Phys. Rev. Lett. **98**, 030401 (2007).

[29] P. Fulde and R. A. Ferrell, Phys. Rev. **135**, A550 (1964); A. I. Larkin and Yu. N. Ovchinnikov, Zh. Éksp. Teor. Fiz. **47**, 1136 (1964) [Sov. Phys. JETP **20**, 762 (1965)].

[30] Studies of the FFLO phase in the imbalanced Fermi gas can be found in recent papers *e.g.*, N.Yoshida and S.-K. Yip, Phys. Rev. A**75**, 063601 (2007) and T. Mizushima, M. Ichioka, and K. Machida, cond-mat/0705.3361, and references therein.

[31] S.-T. Wu and S.-K. Yip, Phys. Rev. A **67**, 053603 (2003).

[32] This sandwiched behavior was also observed for the case of ^{6}Li-^{40}K mixtures, e.g. in reference [23].

[33] Fig 4. of reference [24] missed the structure discussed here.

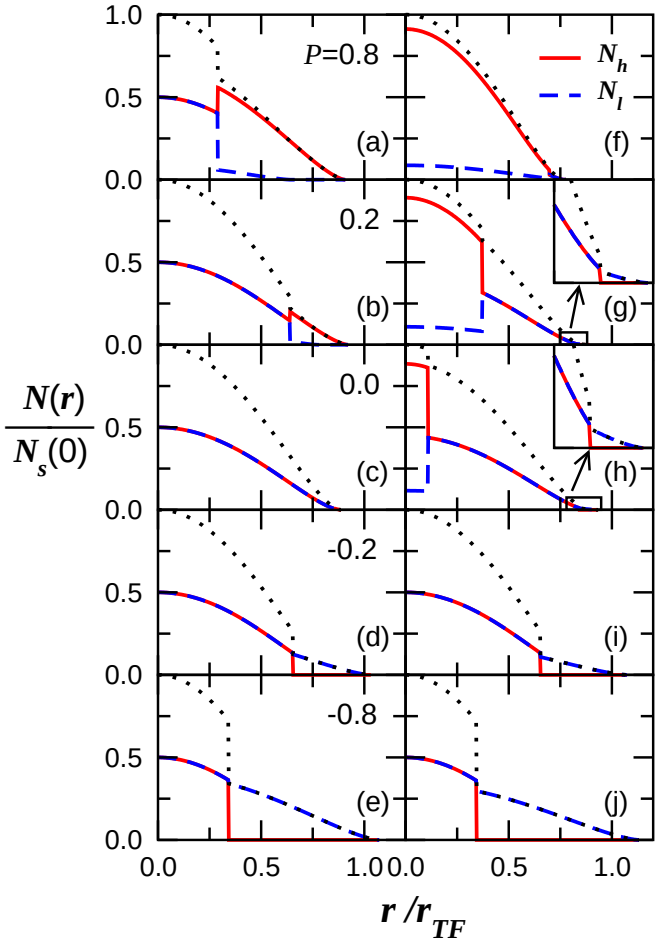

FIG. 1: (Color online) The radial density profiles for heavy fermions (solid lines) and light fermions (dashed lines) at the unitary limit ($(k_F a)^{-1} = 0$). The dotted lines are the total density profiles. The mass ratios γ are equal 2.0 for plots (a)-(e) and 5.0 for plots (f)-(j). The vertical scale is normalized to the total density of fermions at trap center ($N_s(0)$). r_{TF} is the Thomas-Fermi radius of the normal majority cloud.

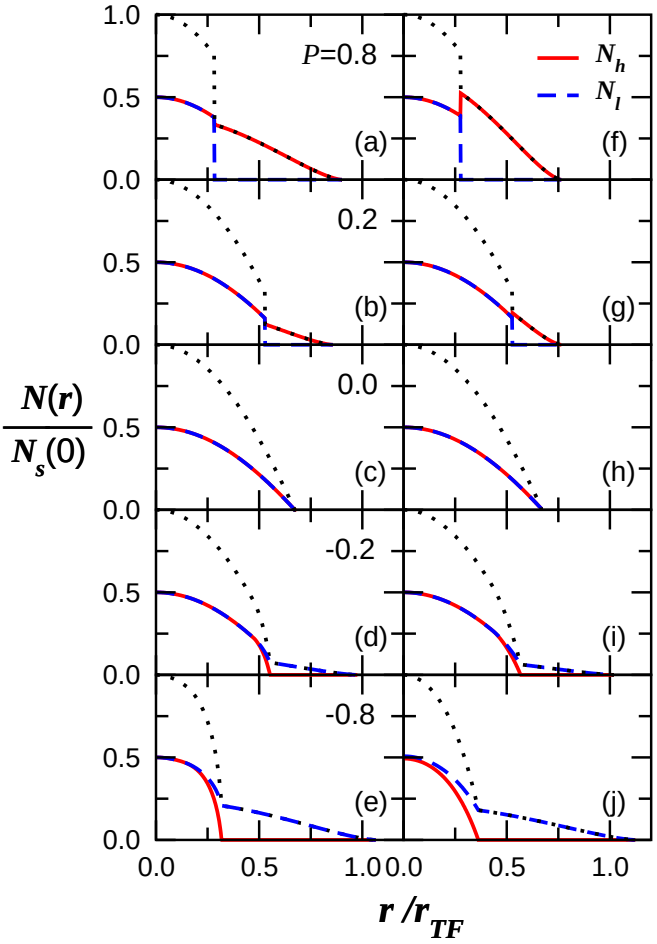

FIG. 2: (Color online) The radial density profiles on the BEC side with $(k_F a)^{-1} = 1.0$. The parameters are the same as in Fig. 1

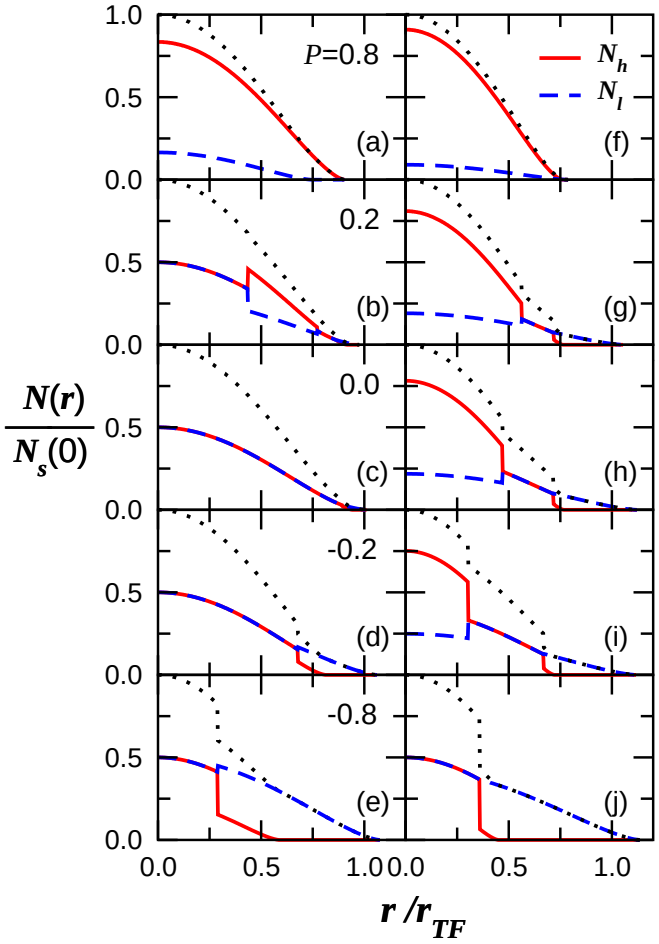

FIG. 3: (Color online) The radial density profiles on the BCS side with $(k_F a)^{-1} = -0.5$. The parameters are the same as in Fig. 1

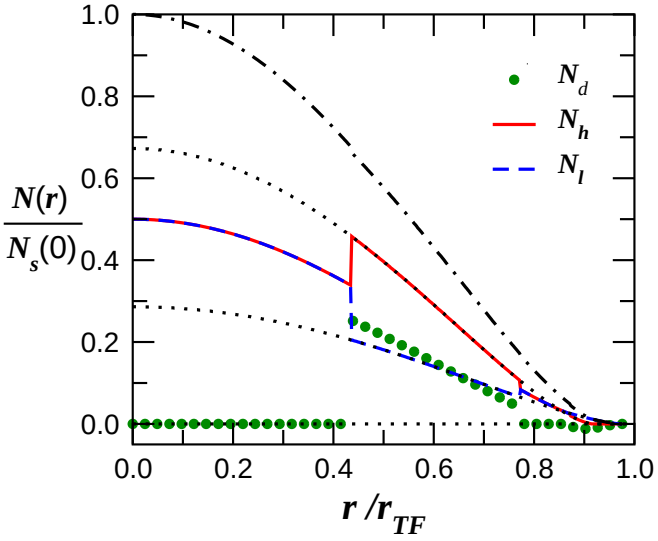

FIG. 4: (Color online) The radial density profiles for heavy fermions (solid lines) and light fermions (dashed lines) with parameters $(k_F a)^{-1} = -0.5$, $\gamma = 2.0$, and $P = 0.2$. The dotted lines are extrapolated density profiles of each component as if they were non-interacting. Solid circles represent the difference between the two components of fermions. Note that, N_d is slightly less than zero near the edge of the trap.

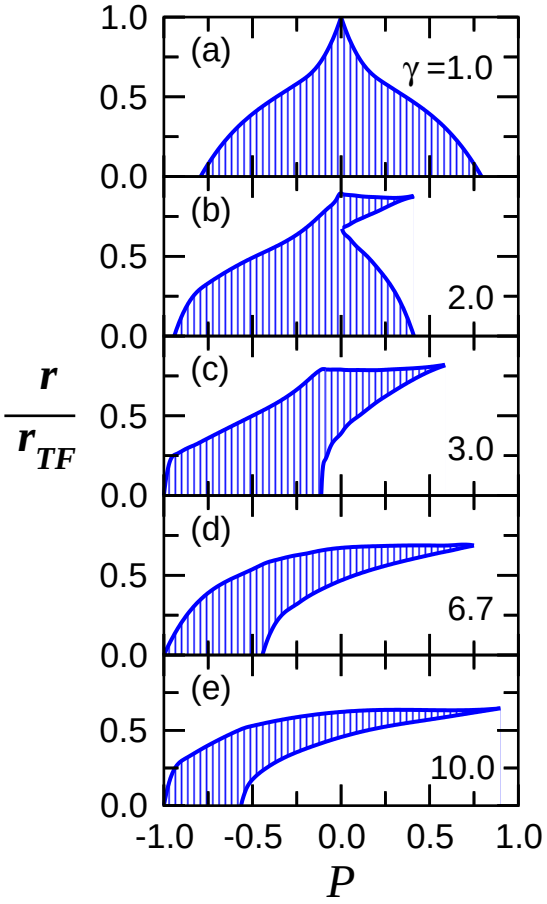

FIG. 5: (Color online) Superfluid phase diagram for $(k_F a)^{-1} = -0.5$ in the trap. The shaded area represents the superfluid phase.

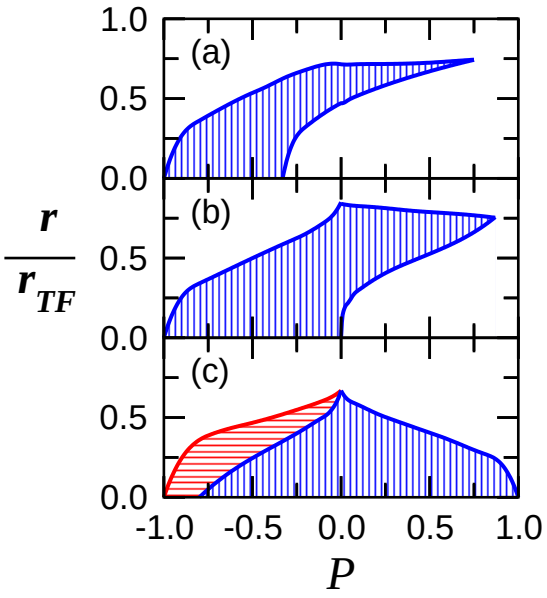

FIG. 6: (Color online) Superfluid phase diagram for $(k_F a)^{-1} = -0.5$ (a), 0.0 (b) and 1.0 (c). The mass ratio $\gamma = 5.0$. The vertical shaded area shows unpolarized superfluid phase and the horizontal shaded area (in plot (c)) shows partially polarized superfluid phase.

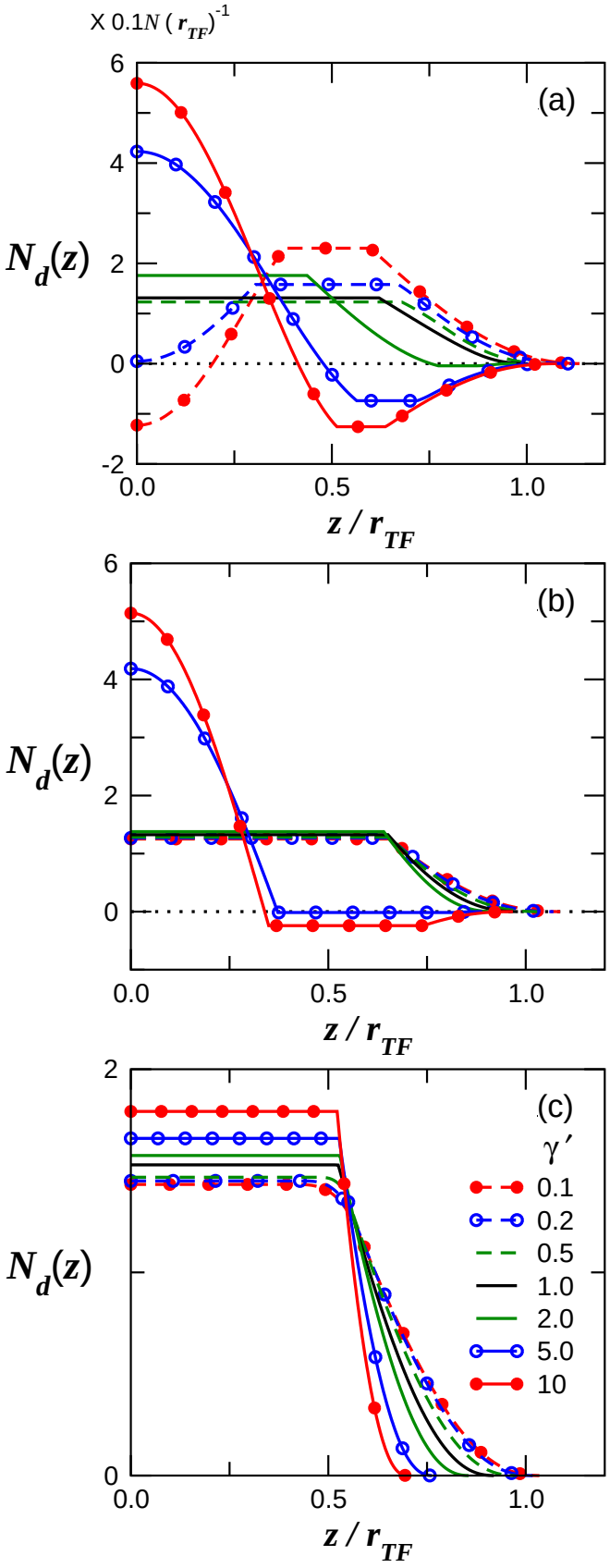

FIG. 7: (Color online) Axial density profiles for $(k_F a)^{-1} = -0.5$ (a), 0.0 (b) and 1.0 (c) with $|P| = 0.2$. Solid lines correspond to the majority heavier ($\gamma' > 1$) and dashed lines corresponding to the majority lighter ($\gamma' < 1$).